Engineered Science
DOI: https://dx.doi.org/10.30919/es917

Evaluation of the Anticorrosion Properties of Passivation Solution Containing Different Metal Ions Coated on a Steel Surface

Yingnan Xu,[1] Liang Yu,[1] Yue Chen,[1] Yu Tian,[1] Chunlin Liu,[1] Junqi Wang, Guangzheng Liu,[1] Yu Bai,[1] Chengxin Guo,[1] Jingchun Liu[1] and Putao Zhang[2,*]

Abstract

The corroded metals in the world account for about 1/3 of the total every year. How to prevent metal corrosion has become a major research topic in the scientific community. Although traditional chromate passivation, phosphate conversion and other technologies can solve the corrosion problem of metals, they pollute the environment and pose a threat to human health. It is urgent to develop new green metal surface treatment technology. The unique chemical structure of silane can form a good protective layer on the metal surface and play an anti-corrosion effect, so the metal surface silanization technology is considered to be the most ideal alternative technology to prevent metal corrosion. Silane passivation solution prepared by organosilicone resin and polyurethane resin mixed with a small amount of metal ions has been used in corrosion prevention of many metals and metal alloys. This study aimed to evaluate the effect of metal ions on the anticorrosion properties of a passivation solution, which contains polyurethane resin and amino silicone resin. Zn^{2+}, Cu^{2+}, and Ni^{2+} were separately added to the passivation solution. This solution was coated on a steel surface using a dip-coating method, and the coated samples were then exposed to 3.5 wt% NaCl solutions for several days. Scanning electron microscopy, thermogravimetric analysis, Fourier transform–infrared spectroscopy, ultraviolet, and electrochemical impedance spectroscopy techniques were conducted to investigate the morphological properties and corrosion resistance of the coatings. The results showed that the types of metal ions were important parameters that affected the corrosion resistance of the coatings. The passivation solution mixed with Zn^{2+} showed better corrosion resistance than that mixed with Cu^{2+} and Ni^{2+}.

Keywords: Anticorrosion; Metal corrosion; Metal ions coating; Surface treatment.
Received: 01 June 2023; Revised: 21 June 2023; Accepted: 28 June 2023.
Article type: Research article.

1. Introduction

The zinc chromate–based passivation solution has been widely used owing to its excellently anticorrosive properties in the past few decades. However, the health and environmental hazards reduced the attractiveness of this solution.[1,2] Silane surface treatment of metals has recently emerged as a promising alternative for chromates in metal-finishing industries. Surface modification and chemical composition of pigments are important parameters affecting corrosion-inhibiting properties.[3] Among organic coatings, polyurethane is one of the most commonly used because it possesses excellent weathering and adhesion properties as well as chemical and abrasion resistance.[4,5] Using polyurethane resin, amino silicone resin, and metal ions that are capable of releasing corrosion-inhibiting species is an important approach to achieve a reliable and long-term corrosion protection performance.[6-8] From the composite coatings, metal ions and resins can participate in anodic and cathodic reactions, that is, the electrolyte diffuses into the metal surface as the immersion time progresses. The results of the cathodic and anodic reactions are $2H_2O + O_2 + 4e^- \rightarrow 4OH-$ and $Fe \rightarrow Fe^{2+} + 2e^-$, respectively. The inhibitive species could react with OH− ions and form insoluble compounds on the steel surface blocking the active sites.[9] As a result, insoluble compounds can be precipitated as a passive layer on the metal surface, providing protection on metal surface against corrosion. The passive layer can block the active zones on the metal surface, causing a decrease in the electrochemical reaction rate.[10,11] The composite coatings in water play a

[1] *Dalian Gaojia Chemical Co. Ltd, Dalian, Liaoning, 116038, China.*
[2] *Key Laboratory of Photovoltaic Materials, Henan University, Kaifeng, Henan, 475004, China.*
**Email:* putaozhang@henu.edu.cn (P. Zhang)

significant role in the anticorrosion of the metal surface.[12]

In this study, Zn^{2+}, Ni^{2+}, and Cu^{2+} were added to the passivation solution, which contained polyurethane resin and amino silicone resin. The solution was coated on the steel surface through a dip-coating method, and the coated samples were then exposed to 3.5 wt% NaCl solutions for several days. The corrosion-inhibiting properties of passivation solutions were investigated using different electrochemical techniques on the steel surface. Scanning electronic microscopy (SEM) was conducted to evaluate the surface morphology of samples coated with passivation solutions and blank steel. Fourier transform–infrared spectroscopy (FT-IR) was carried out to analyze the chemical structure of the composite coating containing Zn^{2+} dried at 120 °C. Thermogravimetric analysis (TGA) and ultraviolet–visible (UV–Vis) absorption spectroscopy were used to characterize the thermal stability of the composite coating and determine the influence of the concentration of passivation solution containing Zn^{2+}, respectively. Moreover, electrochemical impedance spectroscopy (EIS) was performed to examine the corrosion protection properties of steel samples coated with passivation solutions and blank steel

2 Experimental methods

2.1 Materials

Double-[3-(silicon) three oxygen radicals–propyl]-amine (95.6%; 341.55 g·mol^{-1}) was provided by Jing Zhou Jiang Han Chemical Co. (China), and polyurethane resin (30%; 48752 g·mol^{-1}) was provided by Po Tai Chemical Co. (China). The chemical structures of the aforementioned two materials were shown in Scheme 1. Nickle nitrate (98%; 290.81 g·mol^{-1}), copper nitrate (99%; 241.6 g·mol^{-1}), zinc nitrate (99%; 297.49 g·mol^{-1}), sodium chloride (NaCl; 99.5%; 58.44 g·mol^{-1}), and acetone (99%;58.08 g·mol^{-1}) were provided by Its Group Chemical Reagent Co. (China).

Hexafluorozirconic acid (45%; 205.22 g·mol^{-1}) was provided by Shanghai Aladdin Biological Technology Co. (China). Deionized water was produced by HDNRO-1000L Shanghai Gravel Ding Water Treatment Equipment Co. (China). Steel panels (ST-37) were provided by Foolad Mobarakeh Co. (Iran). The quality percentage of various elements of the steel sample ST-37 is shown in Table 1.

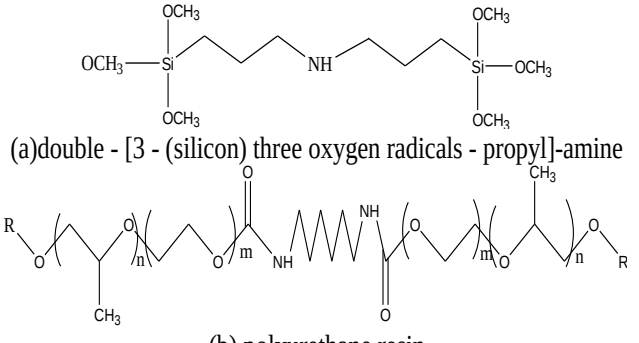

Scheme 1. The chemical structures of (a)double-[3-(silicon) three oxygen radicals-propyl]-amine and (b) polyurethane resin.

2.2 Preparation of passivation solutions and composite coatings

A mixture of 20 g double-[3-(silicon) three oxygen radicals–propyl]-amine in 80 g deionized water was allowed to react for 12 h at room temperature to make sure that silane molecules were sufficiently hydrolyzed, and then 20 wt% amino silicone resin was prepared.

Passivation solutions were prepared by mixing 0.237 g hexafluorozirconic acid (15 wt%), 0.318 g amino silicone resin (20 wt%), 1.537 g polyurethane resin (30 wt%), and 55.687 g deionized water, together with 0.328 g nickel nitrate (6.4 wt%), 0.328 g copper nitrate (6.4 wt%), 0.328 g zinc nitrate (6.4 wt%), or nonmetal ions. The resulting solution was stirred for 10 min. Steel panels were polished with 2000-grit silicon carbide paper, washed with deionized water, degreased using acetone, and dried at room temperature. The samples were dipped in the passivation solutions for 2 min, rinsed with deionized water twice, and dried at 120 ℃ for 30 min. The composite coatings on steel samples were thus prepared

2.3 Techniques

2.3.1 FT-IR analysis

The FT-IR spectrum was recorded using a Spectrum Two FT-IR spectrometer (Perkin Elmer, MA USA) in the range 4000–650 cm^{-1} that determined the chemical structure of the composite coating dried at 120 ℃.

2.3.2 UV analysis

The UV spectrum was recorded on a Cary 60 UV–Vis spectrometer (Agilent, CA USA) that measured the influence of the concentration about the passivation solution containing Zn^{2+}. The sweep range was from 300 to 210 nm. The concentrations of passivation solutions were 0.06, 0.07, 0.08, and 0.09 wt%.

2.3.3 EIS

The EIS was used to evaluate the anticorrosive performance of these composite coatings using an electrochemical workstation PARSTAT 4000 (Princeton, NJ USA). Electrochemical measurements were determined using a three-electrode system: A steel surface coated with different kinds of passivation solutions using a dip-coating method served as the working electrode, while a platinum grid and a saturated calomel electrode served as the counter and reference electrodes, respectively; 3.5 wt% NaCl solutions served as the electrolyte. The EIS measurements were performed at open circuit potential (OCP) on a steel panel of 1 cm^2. The perturbation and frequency range of the measurements were 10 mV and 10^6–10^{-1} Hz, respectively. The polarization test was done at a sweep rate of 1 mV/s in the range of ±100 mV from the OCP.

2.3.4 SEM analysis

The SEM was recorded on a JSM-6510LV model (JEOL, Tokyo), at a voltage of 15 kV to characterize the surface of

Table 1. Chemical composition (wt%) of steel ST-37.

Fe	Mn	Co	Si	C	Cu	Cr	Mo	P	S
97.7	1.39	0.429	0.415	0.19	0.0481	0.026	0.018	<0.005	<0.005

coated and uncoated steel samples.

2.3.5 TGA analysis

The TGA of the composite coating containing Zn^{2+} was recorded on a TG-STDA tool (Mettler Toledo, Switzerland). A sample of approximately 5–10 mg was scanned from 50°C to 700°C at 10°C/min.

3 Result and discussion

3.1 FT-IR analysis

The FT-IR spectrum of the composite coating containing Zn^{2+} dried at 120°C is shown in Fig. 1. The sharp peaks at 2924.99 and 2855.11 cm^{-1} were attributed to symmetric and asymmetric stretching of –CH2–, respectively. The peak at 1739.89 cm^{-1} was due to –C=O, which was from polyurethane resin. The peak at 1531.43 cm^{-1} showed in-plane bending vibration of –NH. The sharp peak at 1248.65 cm^{-1} was due to –C–O–C– stretching. The peak at 1098.72 cm^{-1}, which corresponded to Si–O stretching in –Si–O–Si–, indicated that the condensation reactions occurred among resin themselves in the composite coating. Meanwhile, a broader shoulder detected at 1098.72 cm^{-1} was due to the formation of inorganic Si–O–Zn bonds in the composite coating. The assignments of characteristic absorption bands for the composite coating are summarized in Table 2. The major cross-linking bond of the composite coating was formed when the temperature was 120°C, which was evidenced by the formation of Si–O–Si and Si–O–Zn bonds. A certain amount of uncondensed Si–OH and unhydrolyzed Si–OCH_3 groups remained in the composite coating.[13-20]

Table 2. Infrared absorption of composite coating containing Zn^{2+}.

Bond position (cm^{-1})	Bond assignment	Comment
2924.99	–CH_2	CH stretching
2855.11	–CH_2	CH asymmetric stretching
1739.89	–C=O	C=O stretching
1531.43	–NH	–NH in-plane bending vibration
1248.65	–C–O–C–	C–O stretching
1098.72	–Si–O–Si–, –Si–O–Zn	Si–O stretching
1041.8	–Si–O–CH_3	SiOC stretching

3.2 UV analysis

Figure 2 presents the UV spectrum of the passivation solution containing Zn^{2+} with different concentration. The absorbance was higher and higher with increasing concentration at the wavelength range of 300–210 nm. In particular, the 0.09 wt% concentration showed the highest absorbance at 215 nm. With the result in hand, the change in the concentration of the passivation solution could be monitored.

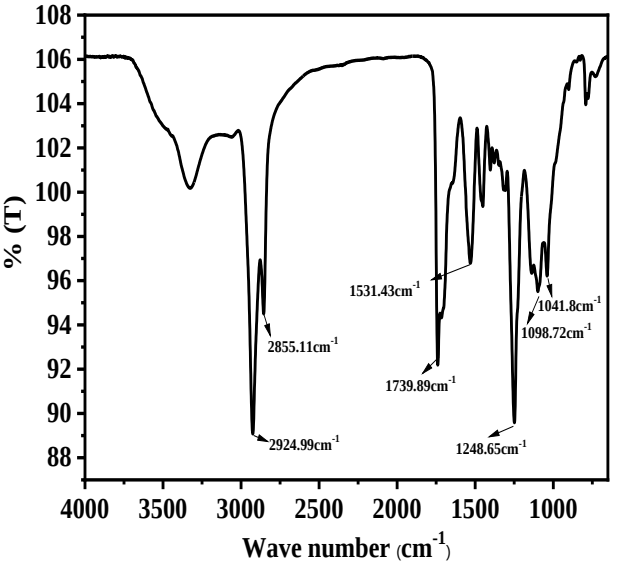

Fig. 1 The FT-IR spectrum of composite coating containing Zn^{2+}.

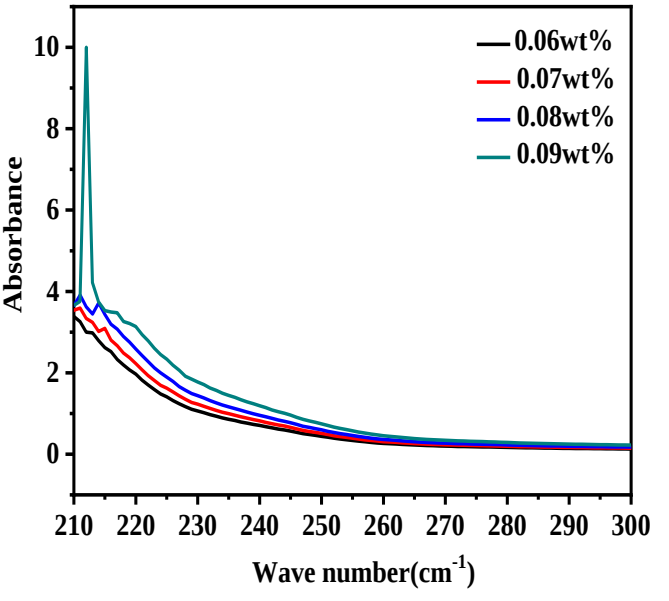

Fig. 2 UV–Vis absorption of passivation solution containing Zn^{2+} at different concentrations

3.3 Corrosion inhibition properties of passivation solutions

3.3.1 OCP measurements

The steel surface was coated with different types of passivation solutions using the dip-coating method. The passivation solutions contained Ni^{2+}, Cu^{2+}, Zn^{2+}, and nonmetal ions. The OCP values of the samples were measured at different immersion times as depicted in Fig. 3. More positive

OCP values were observed in the steel samples coated with passivation solutions containing metal ions compared with the samples coated with nonmetal ions. The most positive OCP values were obtained from the solution containing Zn^{2+} at all immersion times. During the first 1000 s of immersion, the OCP values were negative for all samples. After approximately 2000 s or even longer, the OCP values did not change considerably. These observations indicated that the composite coatings could release inhibitive species in 3.5 wt% NaCl solutions causing restriction of the corrosive species. The passivation solution containing Zn^{2+} showed stronger inhibitory action than those containing other metal and nonmetal ions.

3.3.2 Electrochemical measurements

3.3.2.1 EIS measurements

EIS is a powerful technique used to investigate and predict corrosion-protective performance of coatings. EIS was conducted at a buried electrode/electrolyte interface after stable corrosion conditions were achieved. The four different loops in the Nyquist diagrams (Fig. 4) were of the steel specimen coated with passivation solutions containing Zn^{2+}, Ni^{2+}, Cu^{2+}, and nonmetal ions, after 1, 4, and 24 h of immersion in 3.5 wt% NaCl solutions. Fig. 5 shows the Nyquist diagrams of samples immersed in different types of passivation solutions at 1, 4, and 24 h. As shown in Fig. 4, all samples gradually corroded with longer immersion time, particularly at 24 h.

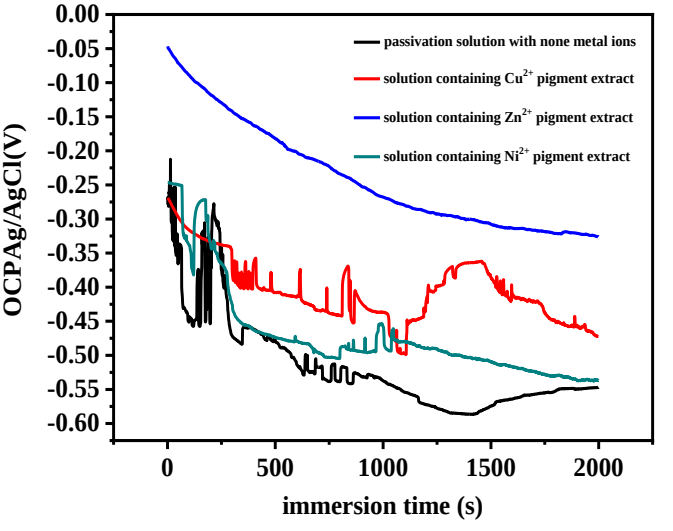

Fig. 3 Variation of OCP *vs* immersion time of the coated steel surface.

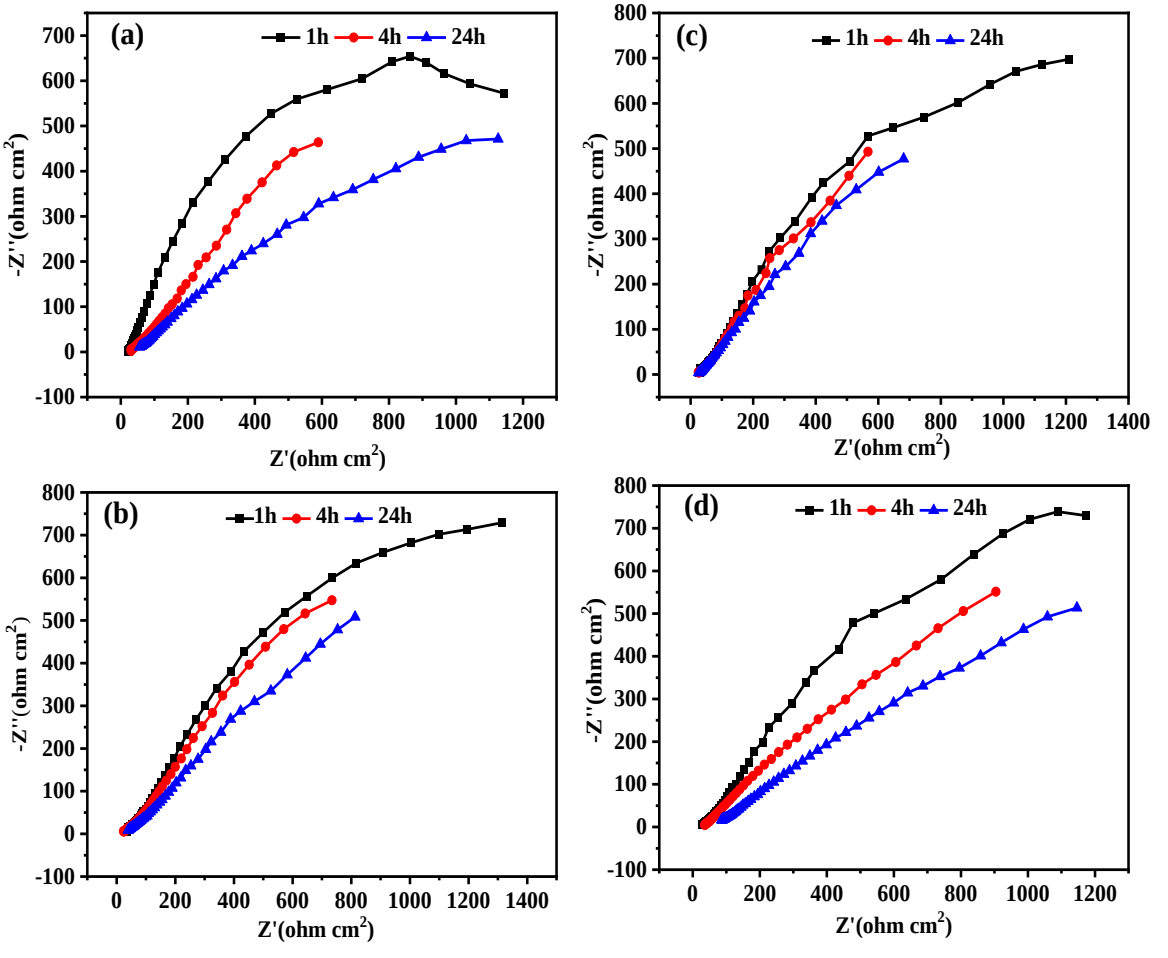

Fig. 4 Nyquist plots of steel samples immersed in 3.5 wt% NaCl solutions. (a) Passivation solution containing Ni^{2+}, (b) passivation solution containing Cu^{2+}, (c) passivation solution containing Zn^{2+}, and (d) passivation solution with none metal ions, at different immersion times.

In Fig. 5, an incomplete semicircle was observed in the high-frequency region, followed by a low-frequency Warburg diffusion tail. The formation of an incomplete semicircle suggested that the NaCl solution had just started permeating through the coating system. Fig. 5 shows that almost none of the samples exhibited any differences at the 1-h immersion time. The differences among the passivation solutions became evident as the immersion time progressed. When the immersion time was 4 and 24 h or even longer, the passivation solution containing Zn^{2+} showed higher resistance toward corrosion compared with the other three coatings. The equivalent circuit model is widely used by numerous researchers for analyzing organic paint systems to protect metals.[21-26] Fig. 6 shows the analysis of the aforementioned EIS spectra. The circuit consisted of a working electrode (steel substrate) and a reference electrode [silver metal (Ag)/silver chloride (AgCl)]. The parameters Rpo (coating pore resistance), Rs (electrolyte resistance), Rp (polarization resistance), Cc (coating capacitance), and Cdl (double-layer capacitance) are generally assumed to be related to the corrosion properties of the system.[27] Rpo is related to the pin hole and coating deterioration, Cc to the water absorption by the coating, and Rp to the polarization resistance of the interface between the coating and steel substrate. Cdl is related to the disbonding of the coating and onset of corrosion at the interface.[28-31] To obtain more precise fitting results, constant phase elements (represented as C) replaced capacitive elements in the equivalent circuit.

3.3.2.2 Polarization test measurements

The effects of passivation solutions containing different types of metal ions on the anodic and cathodic polarization behavior of steels immersed in 3.5 wt% NaCl solutions for 24 h were investigated using polarization measurements. The recorded Tafel plots are shown in Fig. 7. The respective kinetic parameters derived from the plots are provided in Table 3. The data in Table 3 indicate that both anodic metal dissolution of iron and cathodic hydrogen evolution reaction were inhibited

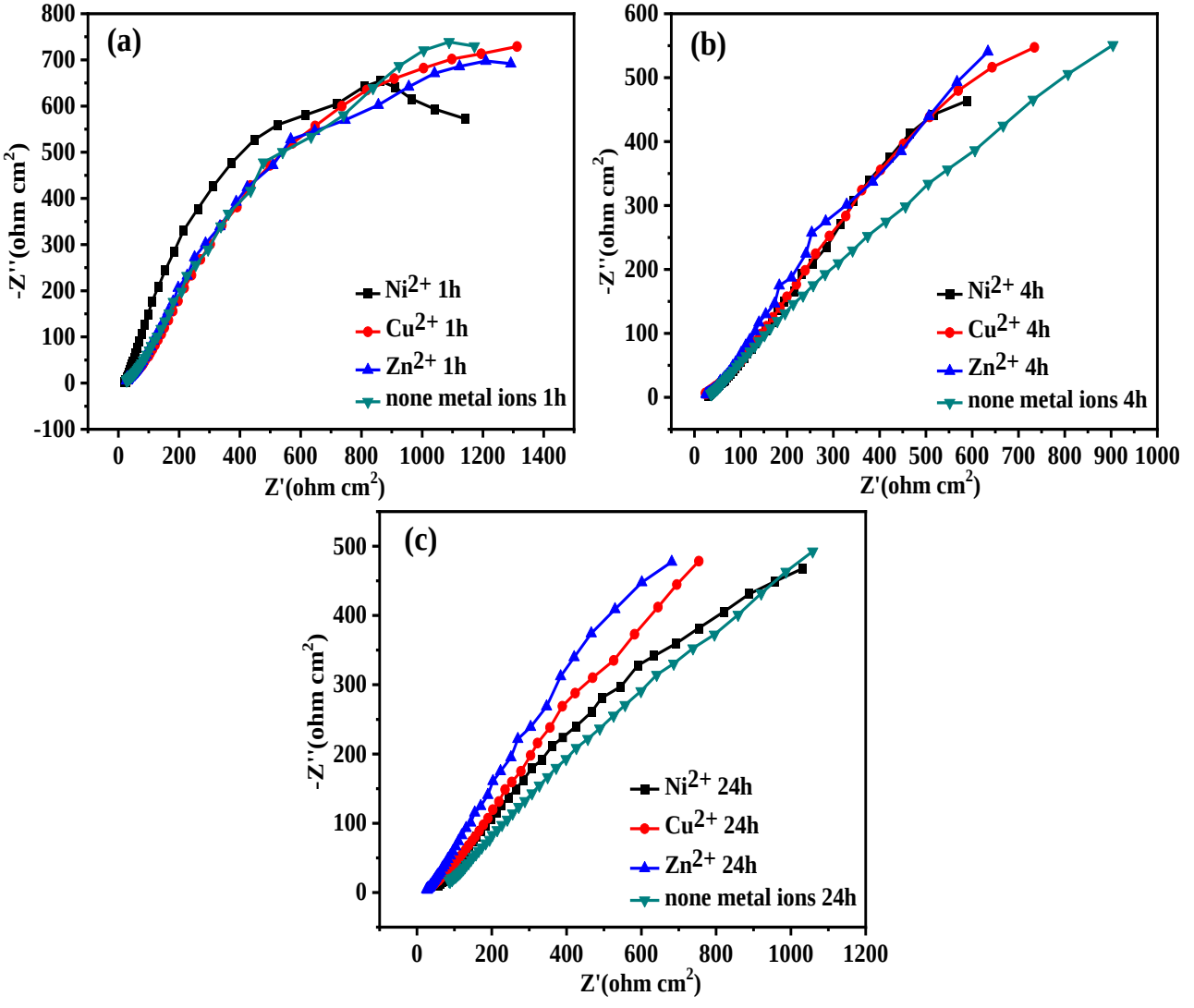

Fig. 5 Nyquist plots of steel samples immersed in 3.5 wt% NaCl solutions for (a) 1 h, (b) 4 h, and (c) 24 h. The steel surface was coated with passivation solutions Ni^{2+}, Cu^{2+}, Zn^{2+} and passivation solution with none metal ions.

Table 3. Corrosion current density, corrosion rate, and polarization resistance for different samples.

Sample	Ecorr[a] vs Ag/AgCl(V)	I_{corr}[b] (μAcm^{-2})	Corrosion rate (mm $year^{-1}$)	ba[c] (V dec^{-1})	bc[d] (V dec^{-1})
Passivation solution containing none metal ions	−0.44	57.64	14.89×10^{-3}	0.27	0.12
Ni2+ passivation solution	−0.31	32.62	26.28×10^{-3}	0.29	1.52
Cu2+ passivation solution	−0.21	15.13	5.53×10^{-3}	0.23	0.15
Zn2+ passivation solution	−0.15	13.52	7.08×10^{-3}	0.12	0.32

[a] The standard deviation range for Ecorr values is between 0.3% and 1.5%.
[b] The standard deviation range for icorr values is between 0.25% and 2.5%.
[c] The standard deviation range for bc values is between 0.7% and 6.0%.
[d] The standard deviation range for ba values is between 1.0% and 6.0%.

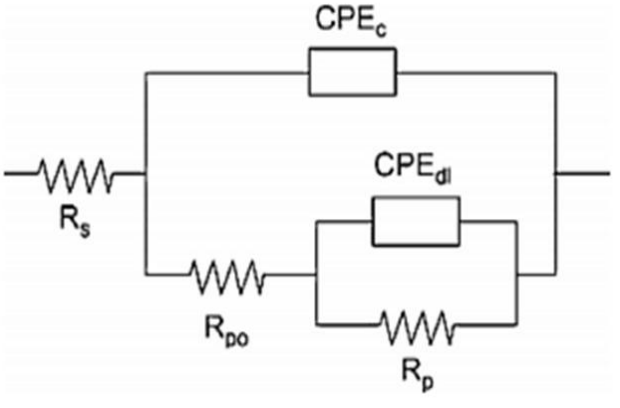

Fig. 6 Equivalent circuit was used to replace EIS impedance data, where passive parameters can be defined. Rs is the electrolyte resistance, Rpo is the pore resistance, Rp is the polarization resistance, CPEc is a constant phase element of the coating capacitance, and CPEdl is a constant phase element of the double layer capacitance.

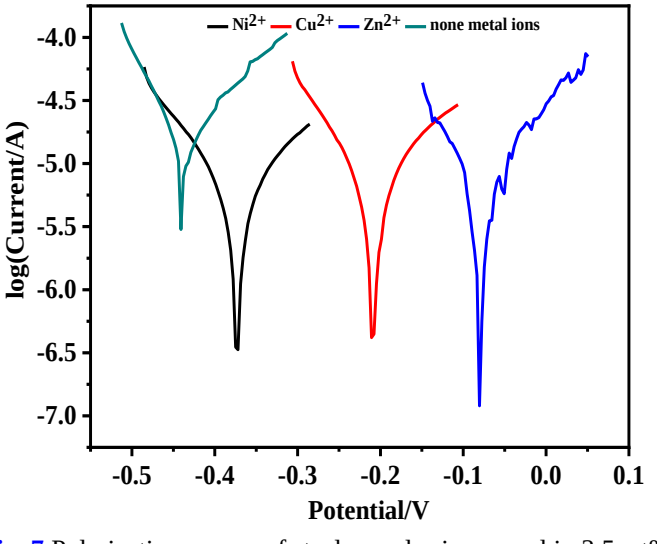

Fig. 7 Polarization curves of steel samples immersed in 3.5 wt% NaCl solutions after 24 h. The steel surface was coated with passivation solutions containing Ni^{2+}, Cu^{2+}, Zn^{2+} and passivation solution with none metal ions.

after the addition of the passivation solutions containing metal ions. Tests were performed to investigate the corrosion inhibition mechanism of the passivation solutions. The electrochemical parameters, including corrosion potential (Ecorr), corrosion current density (icorr), anodic Tafel slope (ba), and cathodic Tafel slope (bc), were derived from the polarization curves (Table 3). Table 3 shows that icorr decreased in the presence of Ni^{2+}, Cu^{2+}, and Zn^{2+}. The decrease in icorr was most pronounced in the dipped specimens. Moreover, Ecorr shifted toward more positive values in the immersed samples. Tests were conducted to investigate the corrosion inhibition mechanism of the passivation solutions containing metal ions. The results showed that the passivation solution containing Cu^{2+} affected the anodic slope more than the cathodic slope. Meanwhile, the passivation solutions containing Ni^{2+} and Zn^{2+} affected the cathodic slope more than the anodic slope. The coating reinforced with passivation solution containing Zn^{2+} showed the best property against steel corrosion.

Figure 8 shows the formation of a small corrosion product on the steel surface panel dipped in the passivation solution containing Zn^{2+} and immersed in 3.5 wt% NaCl solutions after 24 h. The figure clearly reveals that the passivation solution containing Zn^{2+} has higher corrosion inhibition action on the steel surface. In addition, more corrosion product formed on the surface of the steel panel immersed in the passivation solution containing Zn^{2+} compared with the panel containing Ni^{2+}, Cu^{2+}, and nonmetal ions. This result also proved that the passivation solution containing Zn^{2+} significantly improved the corrosion inhibition properties.

3.4 SEM analysis

SEM micrographs (×500) of a blank steel sample and a sample coated with the passivation solution containing Zn^{2+} are presented in Fig. 9. The surface morphology of the blank sample showed numerous pores, cracks, and defects (Fig. 9a). In contrast, the surface morphology of the sample coated with the passivation solution containing Zn^{2+} showed a continuous, dense, and uniform structure (Fig. 9b).

3.5 TGA analysis

The TGA curve of the composite coating containing Zn^{2+} is

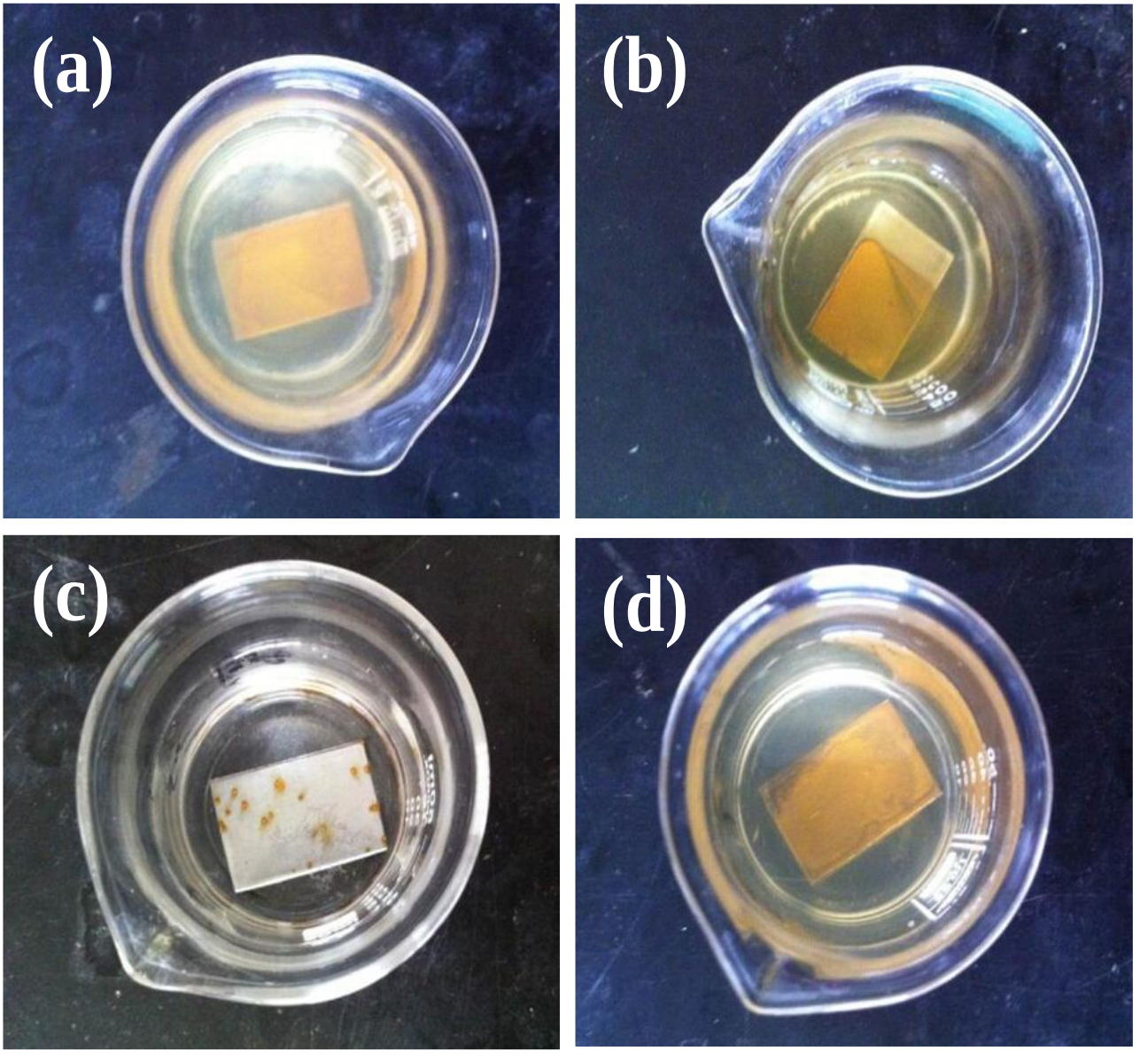

Fig. 8 Visual performance of the samples coated with different passivation solutions dipped in 3.5 wt% NaCl solutions after 24 h. (a)Passivation solution containing Ni^{2+}, (b) Passivation solution containing Cu^{2+}, (c) Passivation solution containing Zn^{2+}, (d) Passivation solution containing none metal ions.

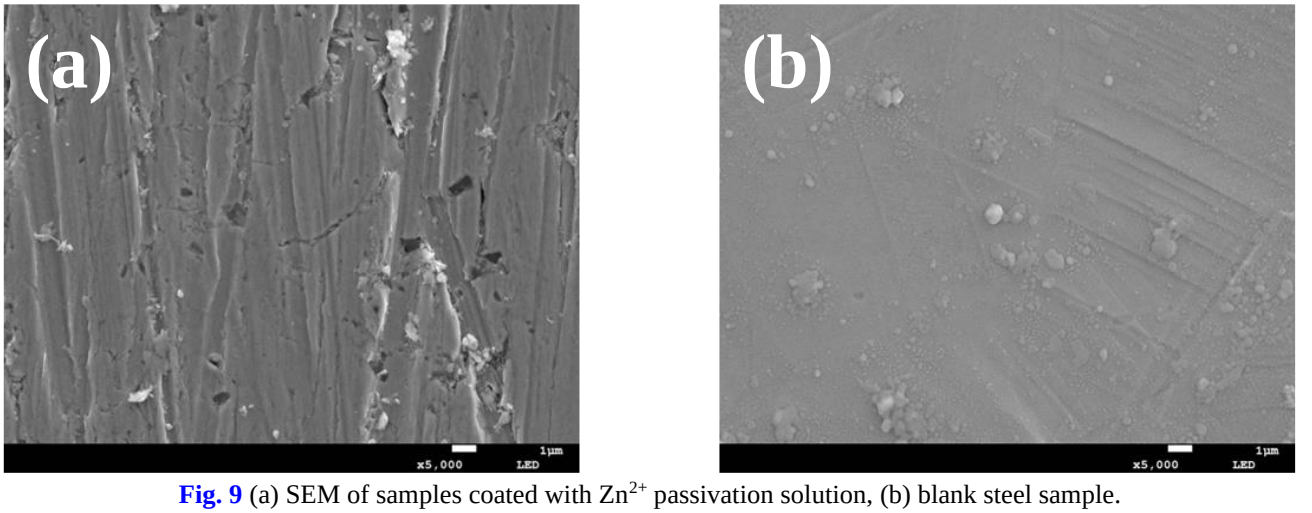

Fig. 9 (a) SEM of samples coated with Zn^{2+} passivation solution, (b) blank steel sample.

given in Fig. 10. A 5% weight loss occurred at the temperature range 50 °C–100 °C because of the loss of absorbed water molecules. The first degradation resulted from the de-cross-linking of C–O and C–C from the resin at the temperature range 150 °C–350 °C. The second decomposition was attributed to the oxidative thermal decomposition of Si–O–Si, Si–OH, and Si–OR at the temperature range 400 °C–450 °C.[32-35] The TGA curves showed that the composite coating containing Zn^{2+} exhibited high decomposition temperature and thermal stability.

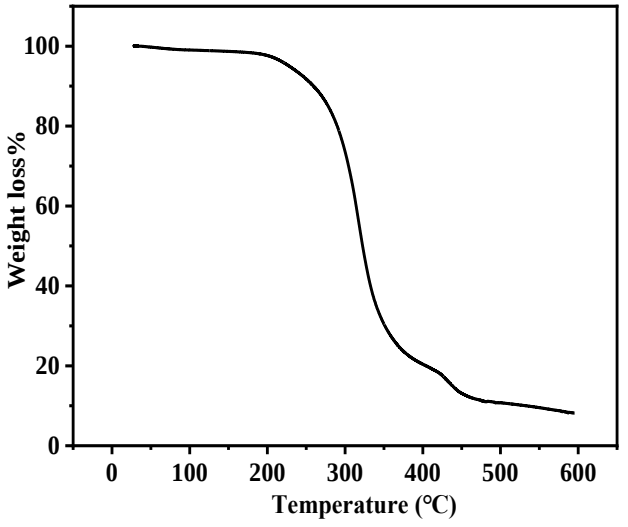

Fig. 10 TGA curve of the composite coating containing Zn^{2}.

4. Conclusions

Different types of metal ions affected the electrochemical properties of the composite coatings. EIS, OCP measurement, and polarization curve revealed that the composite coating containing Zn^{2+} showed higher electrical resistance compared with the other three coatings. The passivation solutions affected both anodic and cathodic reactions. Cu^{2+} exhibited a more prominent effect on the anode reaction rate, whereas Zn^{2+} and Ni^{2+} showed more dominant effect on the cathodic reaction rate. A cross-linking reaction occurred between the composite coating and metal surface covalent bond formation, as proven by FT-IR. UV–Vis showed that absorbance was higher with increasing concentration, especially at a wavelength of 215 nm. The composite coating exhibited high decomposition temperature and thermal stability, which was observed in TGA. A continuous, dense, and uniform membrane was formed on the sample steel surface coated with passivation solution containing Zn^{2+}. This composite coating could prevent the intrusion of corrosion medium, as proven by the SEM images.

Conflict of Interest

There is no conflict of interest.

Supporting Information

Not applicable.

References

[1] R, Naderi, Investigation on the inhibition synergism of new generations of phosphate-based anticorrosion pigments, *Dyes and Pigments*, 2014, **105**, 23-33, doi: 10.1016/j.dyepig.2014.01.015.

[2] R. P. Clark, F. W. Reinhardt, Thermal decomposition of zinc chromates, *Thermochimica Acta*, 1974, **8**, 185-195. doi: 10.1016/0040-6031(74)85085-9

[3] M, Rashvand, Effect of nano-ZnO particles on the corrosion resistance of polyurethane-based waterborne coatings immersed in sodium chloride solution via EIS technique, *Progress in Organic Coatings*, 2013, **76**, 1413-1417, doi: 10.1016/j.porgcoat.2013.04.013.

[4] S. Huang, G. Liu, H. Hu, J. Wang, K. Zhang, J. Buddingh, Water-based anti-smudge NP-GLIDE polyurethane coatings, *Chemical Engineering Journal*, 2018, **351**, 210-220. doi: 10.1016/j.cej.2018.06.103

[5] A. Kausar, Polyurethane nanocomposite coatings: state of the art and perspectives, *Polymer International*, 2018, **67**, 1470-1477. doi: 10.1002/pi.5616

[6] N. Parhizkar, B. Ramezanzadeh, T. Shahrabi, Corrosion protection and adhesion properties of the epoxy coating applied on the steel substrate pre-treated by a Sol-gel based silane coating filled with amino and isocyanate silane functionalized graphene oxide nanosheets, *Applied Surface Science*, 2018, **439**, 45-59, doi: 10.1016/j.apsusc.2017.12.240.

[7] S. K. Dhoke, A. S. Khanna, T. J. M. Sinha, Effect of nano-ZnO particles on the corrosion behavior of alkyd-based waterborne coatings, *Progress in Organic Coatings*, 2009, **64**, 371-382, doi: 10.1016/j.porgcoat.2008.07.023.

[8] S. Y. Arman, B. Ramezanzadeh, S. Farghadani, M. Mehdipour, A. Rajabi, Application of the electrochemical noise to investigate the corrosion resistance of an epoxy zinc-rich coating loaded with lamellar aluminum and micaceous iron oxide particles, *Corrosion Science*, 2013, **77**, 118-127, doi: 10.1016/j.corsci.2013.07.034.

[9] J. Sinko, Challenges of chromate inhibitor pigments replacement in organic coatings, *Progress in Organic Coatings*, 2001, **42**, 267-282, doi: 10.1016/s0300-9440(01)00202-8.

[10] T. J. Harvey, F. C. Walsh, A. H. Nahlé, A review of inhibitors for the corrosion of transition metals in aqueous acids, *Journal of Molecular Liquids*, 2018, **266**, 160-175. doi: 10.1016/j.molliq.2018.06.014.

[11] M. Ganjaee Sari, M. Shamshiri, B. Ramezanzadeh, Fabricating an epoxy composite coating with enhanced corrosion resistance through impregnation of functionalized graphene oxide-co-montmorillonite Nanoplatelet, *Corrosion Science*, 2017, **129**, 38-53, doi: 10.1016/j.corsci.2017.09.024.

[12] A. Kalendová, D. Veselý, J. Stejskal, Organic coatings containing polyaniline and inorganic pigments as corrosion inhibitors, *Progress in Organic Coatings*, 2008, **62**, 105-116, doi: 10.1016/j.porgcoat.2007.10.001.

[13] G. L. Witucki. A silane primer: chemistry and applications of aikoxy silanes, *Journal of Coatings Technology*, 1993, **65**, 57-60.

[14] B. Ramezanzadeh, M. M. Attar, Studying the corrosion

resistance and hydrolytic degradation of an epoxy coating containing ZnO nanoparticles, *Materials Chemistry and Physics*, 2011, **130**, 1208-1219, doi: 10.1016/j.matchemphys.2011.08.065.
[15] B. Xue, T. Yi, D. Li, F. Li, F. Luo. The effect of alkali treatment and organic modification of diatomite on the properties of diatomite composite separators. *New J. Chem.*, 2022, **46**, 23268-23275, doi:10.1039/D2NJ04292D
[16] H. Yao, Z. You, B. Liu, Economic estimation of the losses caused by surface water pollution accidents in China from the perspective of water bodies' functions, *International Journal of Environmental Research and Public Health*, 2016, **13**, 154, doi: 10.3390/ijerph13020154.
[17] L. Abrantes, EQCM study of polypyrrole modified electrodes doped with Keggin-type heteropolyanion for cation detection, *Electrochimica Acta*, 2002, **47**, 1481-1487, doi: 10.1016/s0013-4686(01)00859-3.
[18] T. D. Nguyen, T. A. Nguyen, M. C. Pham, B. Piro, B. Normand, H. Takenouti, Mechanism for protection of iron corrosion by an intrinsically electronic conducting polymer, *Journal of Electroanalytical Chemistry*, 2004, **572**, 225-234, doi: 10.1016/j.jelechem.2003.09.028.
[19] M, Hernández, Effect of an inhibitive pigment zinc-aluminum-phosphate (ZAP) on the corrosion mechanisms of steel in waterborne coatings, *Progress in Organic Coatings*, 2006, **56**, 199-206, doi: 10.1016/j.porgcoat.2006.05.001.
[20] S. H. Zaferani, M. Peikari, D. Zaarei, I. Danaee, J. M. Fakhraei, M. Mohammadi, Using silane films to produce an alternative for chromate conversion coatings, *Corrosion*, 2013, **69**, 372-387, doi: 10.5006/0686.
[21] S. Al-Saadi, R. K. Singh Raman, A long aliphatic chain functional silane for corrosion and microbial corrosion resistance of steel, *Progress in Organic Coatings*, 2019, **127**, 27-36, doi: 10.1016/j.porgcoat.2018.10.024.
[22] Wen, Sun, The role of graphene loading on the corrosion-promotion activity of graphene/epoxy nanocomposite coatings, *Composites Part B: Engineering*, 2019, **173**, 106916, doi: 10.1016/j.compositesb.2019.106916.
[23] S. Ananda Kumar, T. Balakrishnan, M. Alagar, Z. Denchev, Development and characterization of silicone/phosphorus modified epoxy materials and their application as anticorrosion and antifouling coatings, *Progress in Organic Coatings*, 2006, **55**, 207-217, doi: 10.1016/j.porgcoat.2005.10.001.
[24] W.-G. Ji, J.-M. Hu, L. Liu, J.-Q. Zhang, C.-N. Cao, Enhancement of corrosion performance of epoxy coatings by chemical modification with GPTMS silane monomer, *Journal of Adhesion Science and Technology*, 2008, **22**, 77-92, doi: 10.1163/156856108x292287.
[25] R. Naderi, M. Mahdavian, M.M. Attar, Electrochemical behavior of organic and inorganic complexes of Zn(II) as corrosion inhibitors for mild steel: solution phase study, *Electrochimica Acta*, 2009, **54**, 6892-6895, doi: 10.1016/j.electacta.2009.06.073.
[26] M. Rodríguez, The influence of pigment volume concentration (PVC) on the properties of an epoxy coating Part I. Thermal and mechanical properties, *Progress in Organic Coatings*, 2004, **50**, 62-67, doi: 10.1016/j.porgcoat.2003.10.013.
[27] C. Pérez, A. Collazo, M. Izquierdo, P. Merino, X. R. Nóvoa, Comparative study between galvanised steel and three duplex systems submitted to a weathering cyclic test, *Corrosion Science*, 2002, **44**, 481-500, doi: 10.1016/s0010-938x(01)00070-1.
[28] L. Feng, H. Yang, X. Cui, D. Chen, G. Li, Experimental and theoretical investigation on corrosion inhibitive properties of steel rebar by a newly designed environmentally friendly inhibitor formula, *RSC Advances*, 2018, **8**, 6507-6518, doi: 10.1039/c7ra13045g.
[29] D. Loveday, P. Peterson, B. Rodgers, Evaluation of organic coatings with electrochemical impedance spectroscopy, Part 3: Protocols for testing coatings with EIS, *Journal of Coatings Technology and Research*, 2005, **2**, 22-27.
[30] F. Mansfeld, Models for the impedance behavior of protective coatings and cases of localized corrosion, *Electrochimica Acta*, 1993, **38**, 1891-1897, doi: 10.1016/0013-4686(93)80311-M.
[31] A. Amirudin, D. Thieny, Application of electrochemical impedance spectroscopy to study the degradation of polymer-coated metals, *Progress in Organic Coatings*, 1995, **26**, 1-28, doi: 10.1016/0300-9440(95)00581-1.
[32] E. Potvin, L. Brossard, G. Larochelle, Corrosion protective performances of commercial low-VOC epoxy/urethane coatings on hot-rolled 1010 mild steel, *Progress in Organic Coatings*, 1997, **31**, 363-373, doi: 10.1016/s0300-9440(97)00095-7.
[33] Chuansheng, Xiong, Preparation of phytic acid conversion coating and corrosion protection performances for steel in chlorinated simulated concrete pore solution, *Corrosion Science*, 2018, **139**, 275-288, doi: 10.1016/j.corsci.2018.05.018.
[34] G. W. Walter A review of impedance plot methods used for corrosion performance analysis of painted metals, *Corrosion Science*, 1986, **26**, 681-703, doi: 10.1016/0010-938X(86)90033-8.
[35] M. Criado, I. Sobrados, J. Sanz, Polymerization of hybrid organic-inorganic materials from several silicon compounds followed by TGA/DTA, FTIR and NMR techniques, *Progress in Organic Coatings*, 2014, **77**, 880-891, doi: 10.1016/j.porgcoat.2014.01.019.